

Chapter 1

Synthesis of Metallic and Metal Oxide Particles



Kateryna Loza and Matthias Epple

Abstract The diversity of applications in catalysis, energy storage and medical diagnostics utilizes unique and fascinating properties of metal and metal oxide nanostructures. Confined to the nanometer scale, materials may display properties that are different from the equivalent bulk compounds. To meet the requirements for various applications, numerous production techniques were developed to control particle size, morphology, aggregation state, crystal structure, surface charge and composition. This chapter presents an overview of the preparation of metallic and metal oxide nanoparticles by bottom-up and top-down approaches. We describe basic synthetic routes for prominent cases of metals (gold, silver, platinum and copper) and metal oxides (zinc oxide, titania, and silica).

1.1 Introduction

Metal nanostructures attract particular interest because of their unique and fascinating properties compared to their bulk counterparts. The variety of applications comprises biological sensing [1, 2], imaging [3–9], medical diagnostics [10–12], cancer therapy [13, 14], catalysis [15, 16], and energy storage [17, 18]. The observed new chemical, optical, and thermal properties of metallic nanoparticles occur when the size is confined to the nanometer length scale [19]. Numerous techniques were developed to produce metal nanoparticles to meet the requirements for various applications. In general, there are two strategies to manufacture materials on the nanoscale: “Top-down” and “bottom-up” (Fig. 1.1) [20, 21]. The first method is based on breaking down a system (i.e., the bulk material) into smaller units. Common “top-down” techniques are lithography, milling, ultrasound treatment, and laser ablation. These processes

K. Loza (✉) · M. Epple
Inorganic Chemistry, University of Duisburg-Essen, Universitätsstrasse 2,
45141, Essen, Germany
e-mail: Kateryna.Loza@uni-due.de

M. Epple
e-mail: Matthias.epple@uni-due.de

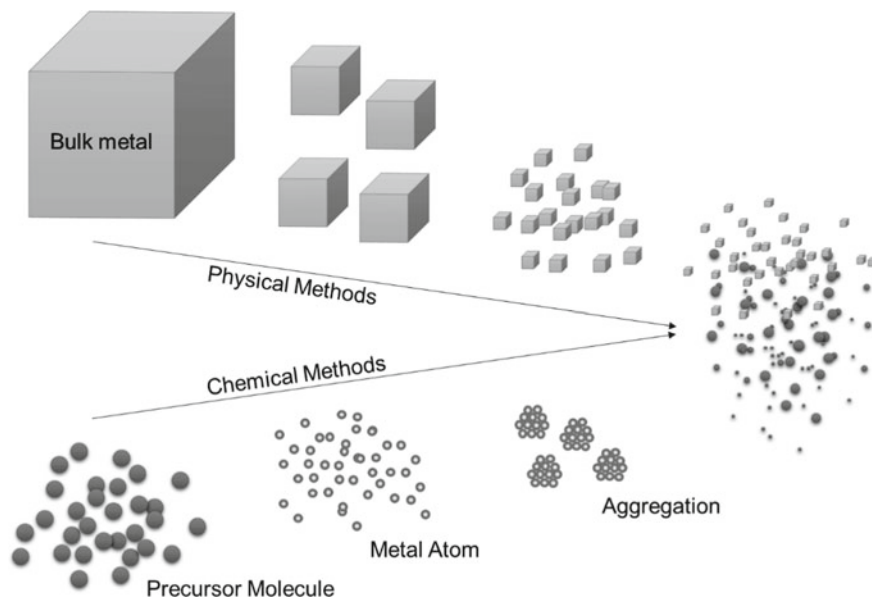


Fig. 1.1 Schematic illustration of synthetic methods for metal nanoparticles. (Adapted with permission from *New J. Chem.*, 1998, 1179–1201. Copyright 1969 The Royal Society of Chemistry) [22]

are comparatively simple and usually lead to ligand-free (“naked”) nanoparticles. However, there is a limited control over the manufacturing process, e.g., an exact size or shape adjustment of resulting particles. The “bottom-up” method relies on material synthesis from atomic or molecular species via a suitable chemical reaction, allowing the particles to grow from smaller units. This approach uses the chemical properties of single molecules or atoms to cause self-organization into the desired particle shape.

The “bottom-up” approach is commonly associated with wet-chemical methods, because colloidal metallic particles are commonly produced by chemical reduction of metal salts dissolved in a suitable solvent in the presence of surfactants or ligands that cover the surface [23]. A wide range of reducing agents have been used in the colloid-chemical synthesis of metal nanoparticles [24]. For example, H_2 , hydrazine, hydroxylamine, hydrides (e.g. $NaBH_4$ or B_2H_6), ascorbic acid or ascorbate, citric acid or citrate, reducing polymers (e.g., PVA) and solvents (like alcohols, diols, aldehydes, and DMF) have been used to prepare metal nanoparticles [25–29]. Reduction can take place at room temperature or at elevated temperatures, depending on the relative reduction potentials of the precursor and the reducing agents [30–33].

In the following, we discuss the cases of gold, silver, copper, and platinum as representative examples, and also the preparation of alloyed nanoparticles by various synthetic methods. The described methods can typically be transposed to other kinds of nanoparticles, typically of noble metals.

1.2 Metals (Gold, Silver, Platinum and Copper)

1.2.1 Gold

The first systematic synthesis of Au colloids was reported 160 years ago by Michael Faraday using phosphorus to reduce AuCl_4^- ions [34]. In the 1950s, an easier approach was established and standardized by Turkevich [35]. He used the mildly reducing agent trisodium citrate, added to a boiling aqueous solution of HAuCl_4 , to obtain monodisperse gold nanoparticles in the size range from 10 to 40 nm. Due to its simplicity, this synthetic method was adapted in many variations [36, 37]. For example, switching to a mixture of reducing agents (e.g. citrate and tannine) allows to clearly shorten the reaction time and to enhance the stability of the formed colloid [38, 39].

The reduction of tetrachloroauric acid in an aqueous medium is a versatile synthetic route and possible with many different reducing agents like sodium borohydride (NaBH_4), ascorbic acid, and hydroquinone [40–42]. The use of NaBH_4 as reducing agent results in a fast reduction and a gold particle size of 1–5 nm [29, 43, 44]. In general, the choice of the reducing agent has a strong influence on the resulting particle size, since with increasing reduction potential the number of the formed nuclei increases and the growth of particles is limited. On the nanometer scale, metals tend to nucleate and grow into multiply twinned particles with their surfaces defined by the lowest-energy facets [45]. Anisotropic gold nanoparticles (rod-, rectangle-, hexagon-, cube-, triangle- and star-like shapes) with less stable facets were kinetically achieved by adding chemical capping reagents, i.e. agents that selectively block certain crystal faces, to the reaction mixture [25, 46, 47].

The previously described methods are based on a synthesis from atomic or molecular species by chemical reaction, so called “bottom-up” approach. In liquid media, dispersed metallic nanoparticles can be generated by the pulsed laser ablation process, a “top down” technique [48]. This method provides ligand-free nanoparticles [49]. The size of obtained particles can be varied to some extent by the laser parameters and by subsequent laser fragmentation steps [50, 51]. Furthermore, an in situ conjugation of nanoparticles with biomolecules by laser ablation in an aqueous medium is a highly promising one-step method for the production of functional nanoparticles [52].

The polydispersity of nanoparticles is a key concern in nanoscience research. Even though reasonably monodisperse nanoparticles can be produced, usually not all nanoparticles are fully identical (see Fig. 1.2 for an example). This fact leads to the ultimate aim for a synthesis of atomically precise nanoparticles [53]. In the case of gold, this was accomplished for ultrasmall gold nanoparticles (containing 10–300 atoms, often called nanoclusters) [54, 55]. Several groups established synthetic routes to produce a gold core in the size range of 1–3 nm. Such ultrasmall nanoparticles are typically formed by metal salt reduction in the presence of phosphanes (PR_3) [56, 57] or thiols (HS-R) [44]. Exerting a strict control over the size of a cluster strongly affects the activity and the selectivity in a catalytic process [58]. Furthermore, a

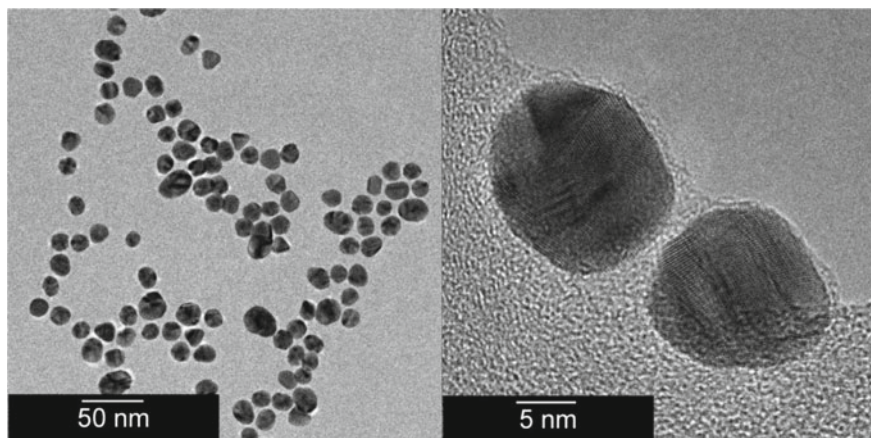


Fig. 1.2 Transmission electron micrographs of PVP-stabilized gold nanoparticles, prepared by the standard citrate method after Turkevich. (Reproduced from the dissertation of D. Mahl, 2011, University of Duisburg-Essen) [60]

supracolloidal self-assembly of atomically precise nanoparticles is a promising platform for novel 2D and 3D materials with additional plasmonic functionalities, novel mechanical properties, and inherent flexibility [59].

1.2.2 Silver

Colloidal silver is known since about 120 years [61]. The manufacturing of silver nanoparticles can be done by physical processes such as ultrasonication, chemical vapor deposition, or pulsed laser ablation in liquids [62–64]. However, wet-chemical “bottom-up” syntheses offer more possibilities for the variation of particle size, morphology and functionalization. The most commonly used precursor for preparing silver nanoparticles in wet-chemical reductions is silver nitrate (AgNO_3) because of its high solubility in many polar solvents and dispersability in less polar solvents, sometimes after adding surfactants and/or using ultrasonication. The reducing agents used in the synthesis of nanoparticles from silver(I) ions are comparable to those used for gold nanoparticle preparation. Already in 1889, M. C. Lea published the synthesis of citrate-stabilized silver nanoparticles [65]. In general, one-pot methods for the reduction of silver nitrate have evolved, where different reducing agents such as sodium citrate [66], glucose [67], ascorbate [68], sodium borohydride [69, 70], polyols [71, 72], and ammonium formate were used [73]. Typically, the reactions are performed at elevated temperatures by conventional heating in an oil bath. Alternatively, microwave-assisted syntheses can increase the reaction rates and yields as well as selectivity and reproducibility [30].

The particle properties depend not only on their size but also on their morphology. As a result, a shape-controlled synthesis of silver nanoparticles is of special

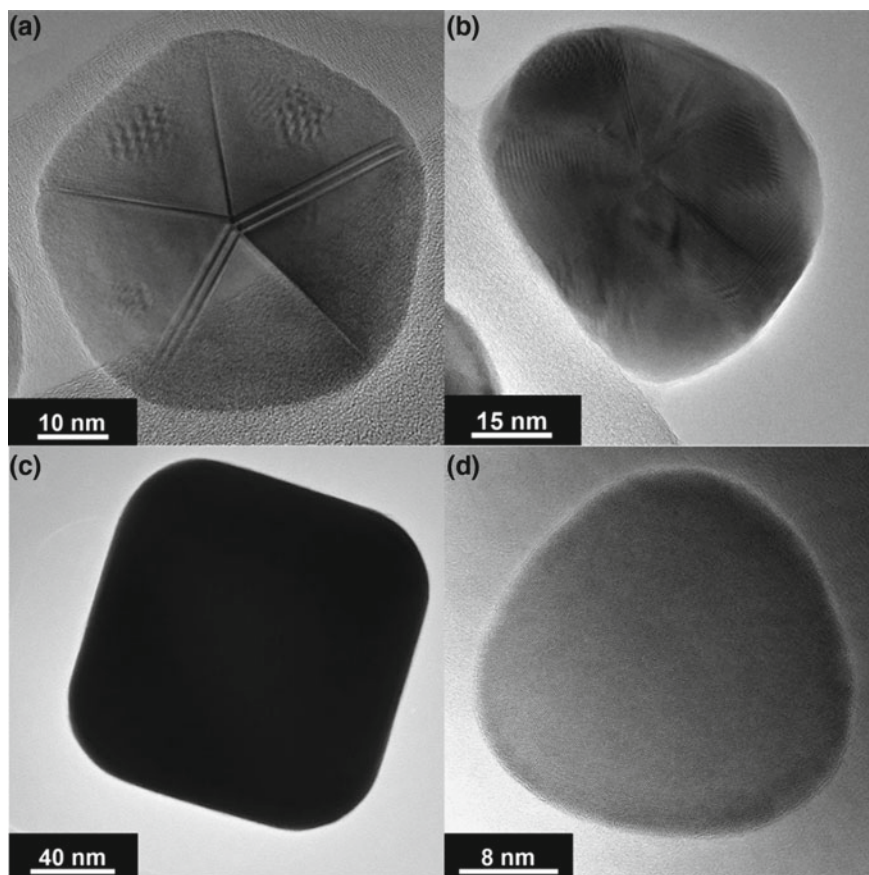


Fig. 1.3 Transmission electron micrographs of different kinds of PVP-stabilized silver nanoparticles, prepared by glucose reduction (a) [67], a microwave-assisted reduction (b) [30], a modified polyol synthesis (c) [79], and a microwave-assisted modified polyol process (d) [80]. (Adapted with permission from *Cryst. Growth Des.* 16, 7, 3677–3687. Copyright 2016 American Chemical Society) [81]

interest. Xia et al. and others described the structural evolution of silver nanoseeds to nanoparticles with defined shapes like platelets [74], cubes [75], rods [76], rings [77], and bipyramids [78] (Fig. 1.3).

It is critical to understand not only the growth mechanism of nanostructures, but the process of seed formation, because the number of twin planes in the initial stage is the key factor for determining the shape of the final product (single-crystal seeds form cubes, multiply-twinned decahedral seeds form wires) [82].

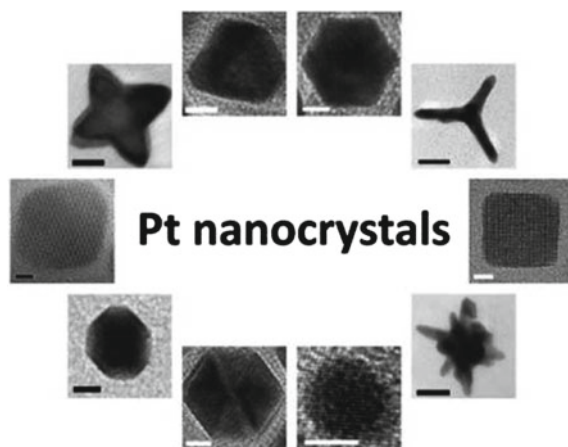


Fig. 1.4 Transmission electron micrographs of platinum nanoparticles, prepared by solution-phase synthesis using metal carbonyls as reducing agents. This synthetic method produces highly monodisperse Pt octahedral, icosahedra, cubes, truncated cubes, cuboctahedra, spheres, tetrapods, star-shaped octapods, multipods, and hyper-branched structures. (Reproduced with permission from ACS Nano 7, 1, 645–653. Copyright 2012 American Chemical Society) [89]

1.2.3 Platinum

Platinum nanostructures are of particular interest for many industrial applications due to their extraordinary catalytic properties in various industrial syntheses like petrochemistry or energy conversion [83–86]. Conventional techniques to prepare platinum nanoparticles are based on wet-chemical methods [87–89]. Typically, the reaction involves the reduction of a Pt(II) precursor (like K_2PtCl_4 or $\text{Pt}(\text{acac})_2$) or a Pt(IV) precursor (like K_2PtCl_6) in the presence of a stabilizing polymer by reducing agents such as hydrogen [90], carbon monoxide [91], sodium borohydride [92], lithium borohydride [93], and ethylene glycol [94]. The resulting nanoparticles may be considered as monodisperse in size, but they are often irregular in shape and lack well-defined facets [95]. Further modifications may include sonication during the reaction [96] or microwave-assisted heating [94]. Because the reactivity and the selectivity of Pt nanoparticles are highly dependent on the exposed facets [97], the synthesis of uniformly shaped particles is decisive for high catalytic performance [98]. Their morphological evolution is often controlled by the reduction kinetics of the platinum precursor [95], the reaction temperature [98], or the use of shape-directing reagents [99, 100] (Fig. 1.4).

The previously syntheses were based on the “bottom-up” approach. However, chemical synthesis methods often lead to impurities of the nanoparticle colloids caused by additives and precursor reaction products [101]. In contrast, Barcikowski et al. demonstrated the preparation of ligand-free platinum nanoparticles by laser

ablation in liquids (“top-down” technique) for the surface modification of electrodes for neural stimulation [102].

1.2.4 Copper

Since the ninth century, copper nanoparticles are known as coloring agents in Mesopotamia [103]. Nowadays the application range comprises biomedicine [104, 105], sensors [106], conductive inks [107], and organic catalysis [108–110]. Being inexpensive and rather abundant in nature, copper is utilized in large scale for the fabrication of plasmonic solar cells [111]. Recently established methods for copper nanoparticle synthesis include laser ablation [112], thermal decomposition [113], the polyol process [114, 115], and other chemical reduction methods [116]. Typical precursors for copper nanoparticle wet-chemical syntheses are CuSO_4 , copper acetylacetonate ($\text{Cu}(\text{acac})_2$), CuCl_2 , and $\text{Cu}(\text{NO}_3)_2$ [117]. Reducing agents comprise ascorbic acid [118], sodium borohydride [119], and hypophosphite [120]. It should be mentioned that the preparation of Cu nanoparticles is challenging due to its high sensitivity to air because copper is easily oxidized to copper oxides, being less noble than silver, gold, or platinum metals [121]. The oxidation of copper nanoparticles can be avoided if the synthesis is conducted in non-aqueous media (sometimes under inert gas) and in the presence of CO or H_2 . Previously described synthetic routes result in spherical multi-twinned nanoparticles in the size range between 10 and 70 nm. As shown in Fig. 1.5, by variation of the ratio of copper acetylacetonate to oleylamine, different particle size distributions can be achieved. If a hydrothermal treatment is applied, anisotropic copper particles such as nanowires or nanorods can be produced [110].

1.3 Alloyed Nanoparticles

The properties of metallic systems can be significantly extended by mixing elements to generate intermetallic compounds and alloys. Due to synergetic effects, an enhancement in desired properties is possible. The diversity of compositions, structural organizations, and tunable properties of metallic alloys makes them suitable for a wide range of applications in electronics, engineering, biomedicine, and heterogeneous catalysis [123–126]. For example, alloyed silver and gold nanoparticles utilize the physicochemical properties of both metals, e.g., the optical properties of gold and the toxicity towards bacteria or cells of silver [127, 128]. Surface structure, composition, and segregation properties [129] of nanoalloys are of great importance for the chemical reactivity and the selectivity in catalysis [130, 131]. If confined to the nanometer scale, they may display properties that are different from the equivalent bulk compounds. For example, iron and silver are immiscible in the bulk, but can be mixed in nanoparticles [132] (Fig. 1.6).

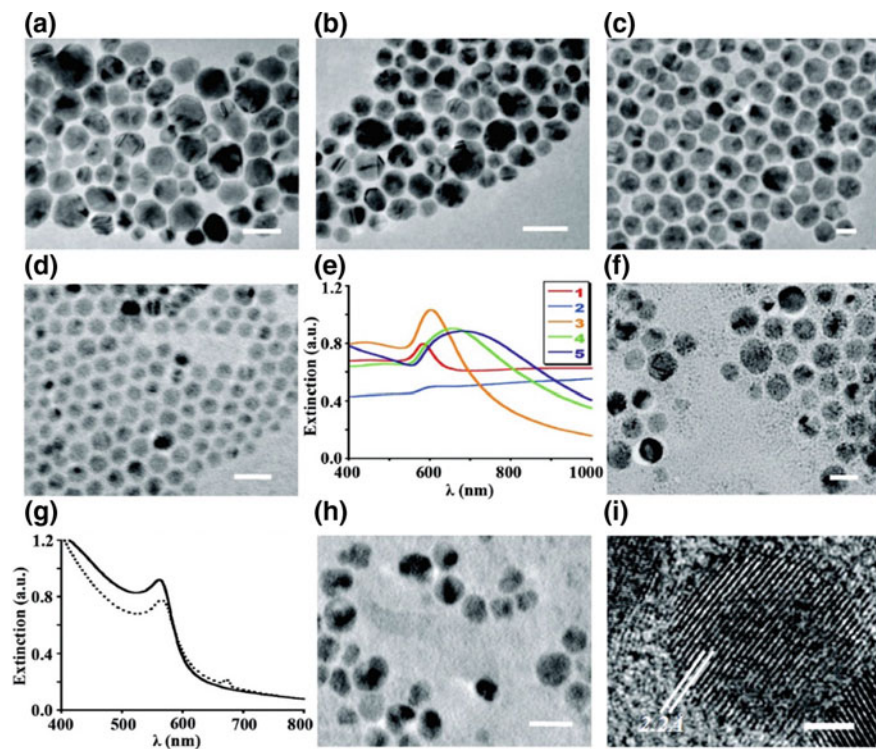


Fig. 1.5 Transmission electron micrographs and UV/VIS spectra of copper nanoparticles, prepared with different ratios of copper acetylacetonate and oleylamine. Scale bars in **a** and **b** are 50 nm, those in **c**, **d**, **f**, and **h** are 20 nm, and that in **i** is 2 nm. (Reproduced with permission from *J. Phys. Chem. C*, 2010, 114 (37), pp 15612–15616. Copyright 2010 American Chemical Society) [122]

Due to the heterogeneity of different properties of individual components (e.g., crystal system, redox potential, crystal symmetry, or surface charge), the successful mixture of these materials into a finite nanoparticle is challenging [123, 133]. In general, the methods for preparation of nanoalloys are the same as for single metal nanoparticles. Ligand-free manufacturing methods of nanoparticles are based on laser ablation of solids in liquid environment [134, 135], pulsed arc discharge, and sputtering techniques [123]. These approaches start with single, bimetallic or ternary targets or mixed metallic powders. Figure 1.7 shows a typical setup and the obtained alloyed Ag/Au nanoparticles by laser ablation in liquids.

Bimetallic colloids can be generated by chemical reduction of a suitable mixture of salts (metal precursor) in the solution, using appropriate reducing agent. To avoid the formation of core-shell structures due to the difference in redox potentials, different ligands can be used [137]. Another variation is based on the reduction of double metal complexes [22]. Instead of chemical reduction, an electrochemical process can be

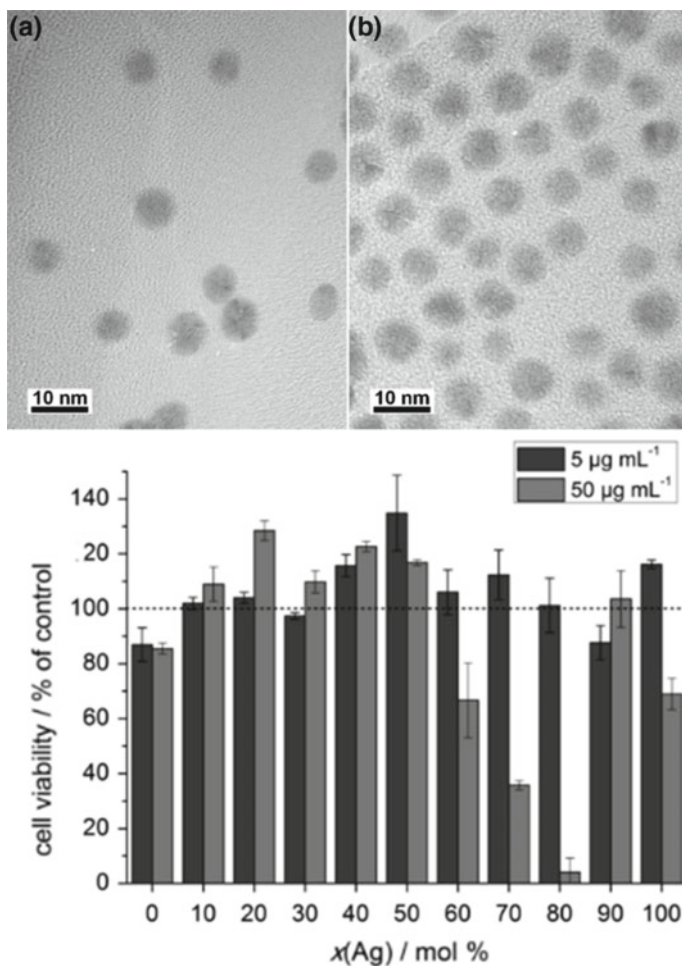


Fig. 1.6 Transmission electron micrographs of PVP-functionalized Ag/Au alloyed nanoparticles and the viability of HeLa cells after incubation with alloyed nanoparticles. Note that the cytotoxicity is not proportional to the relative silver amount, pointing to special effects that occur in the alloyed nanoparticle beyond a mere additivity of the metal properties. (Adapted from Beilstein J. Nanotechnol. 2015, 6, 1212–1220; © 2015 Ristig et al.; licensee Beilstein-Institut) [127]

used to create metal atoms from bulk metal. The particle size was controlled by the current density [138].

Seeded-growth techniques permit the synthesis of core-shell nanoparticles [139]. As seen from Fig. 1.8, Pd–Au core-shell nanoparticles can be prepared by a water-based one-pot synthesis, followed by a stabilization with poly(*N*-vinyl pyrrolidone). Here, a sequential metal deposition with a distinct boundary between both metals was achieved [140].

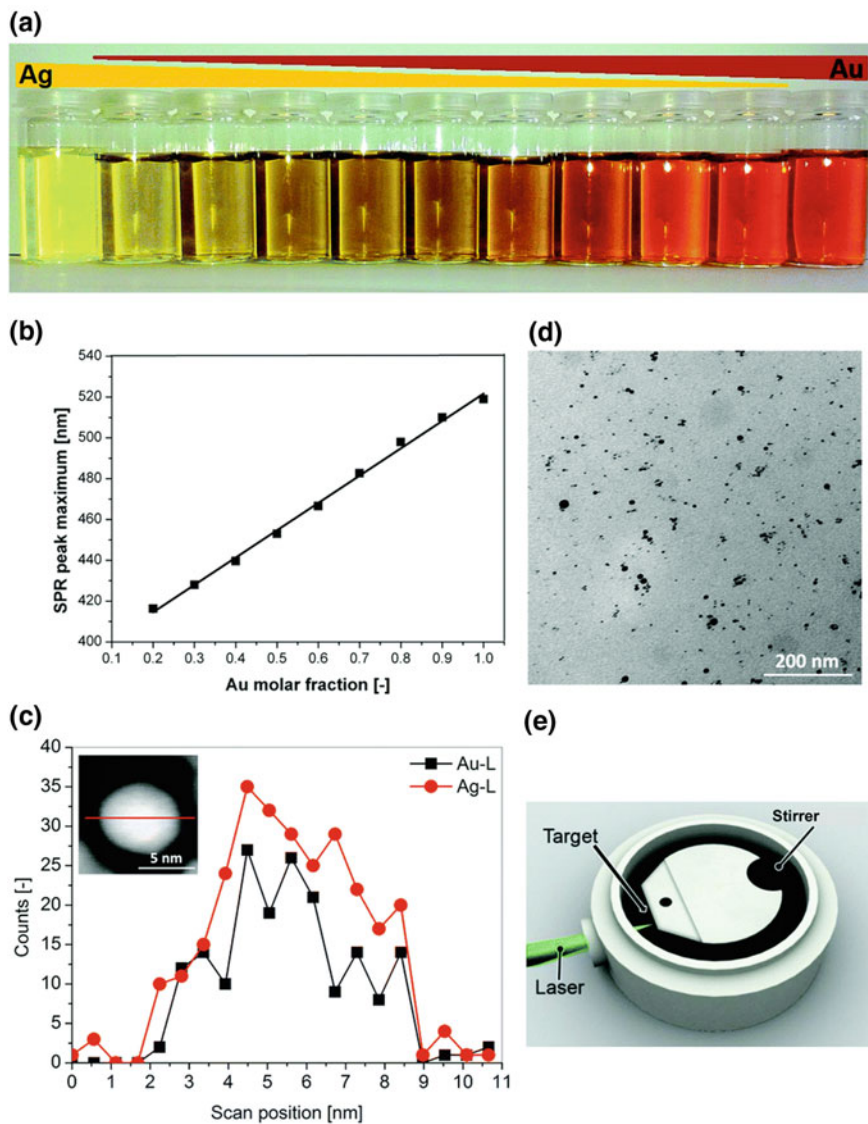


Fig. 1.7 **a** Representative AuAg nanoparticles with different molar fractions. **b** Correlation of the gold molar fraction with a maximum surface plasmon resonance extinction peak. **c** TEM-EDX line scan with an inset, showing a high-angular annular dark field micrograph. **d** TEM micrograph of Ag₅₀Au₅₀ nanoparticle dispersion after stabilisation with BSA. **e** Aluminum batch chamber for the synthesis of silver and gold-silver alloyed nanoparticles. (Reproduced with permission from Analyst, 2014, 139, 931–942. Copyright 2014 The Royal Society of Chemistry) [136]

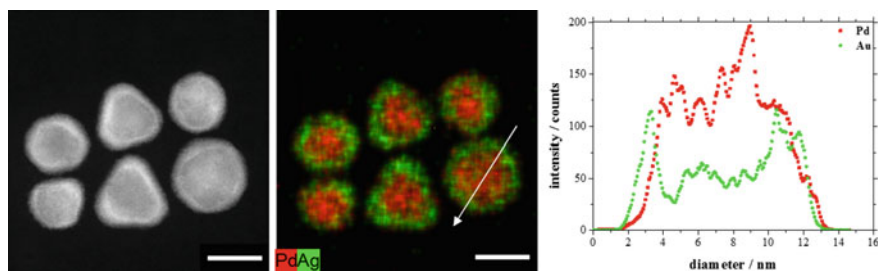


Fig. 1.8 HAADF-STEM image and corresponding EDX map with an additional line scan (white arrow) of Pd–Au core-shell nanoparticles. The EDX maps and line scans clearly show the presence of a core-shell structure with a palladium core (red) and a gold shell (green). The scale bars are 7 nm. (Reproduced with permission from ChemistrySelect 2018, 3, 4994. Copyright 2018, John Wiley and Sons)

The synthesis of alloyed nanoparticles with non-spherical morphology can lead to specific optical properties like plasmonic resonances and surface-enhanced Raman scattering (SERS) [141, 142].

1.4 Nanoscale Oxide Particles

Due to their intrinsic properties, metal oxide nanoparticles strongly contribute to a variety of applications in chemistry, physics, and materials science [143, 144]. A large diversity of oxide compounds with many structural geometries and various electronic structure (metals, semiconductors, or insulators) is known. They are widely applicable in the fabrication of sensors [145], microelectronic circuits [146], piezoelectric devices [147], fuel cells [148, 149], passivation coatings [150], water treatment agents [151], bactericides [152], sun screen [153], and as heterogeneous catalysts [154]. Almost all active phases, promoters, or “supports” in industrial catalytic reactions are based on oxides. The entanglement of size, shape, morphology, crystal structure, and surface chemistry requires a fundamental understanding and rational design for technologically relevant areas. In the following, we will discuss the prominent cases of zinc oxide, titanium dioxide (titania), and silicon dioxide (silica).

1.4.1 Zinc Oxide Nanoparticles

Zinc oxide (ZnO) is extensively utilized in everyday applications, like transparent electronics, smart windows, piezoelectric devices, chemical sensors, biosensors and dye-sensitized solar cells [155, 156]. However, zinc oxide is used at least since 2000 BC as component of therapeutic creams for skin medication [157]. Registered as safe material by the Food and Drug Administration (FDA) [158], it is used as food additive and inorganic antimicrobial additive in polymeric matrices for the packaging material, e.g. the incorporation of ZnO into the coatings of containers for meat, fish, corn and peas can retain the food color and avoid degradation [159]. Today, the commercial production of ZnO nanoparticles is realized by mechanochemical processing and physical vapor synthesis [160]. The first method is based on physical size reduction in a conventional ball mill with additives that are activated during grinding. The reaction comprises the mechanical activation of precursors (ZnCl_2 and Na_2CO_3) with a further thermal decomposition to ZnO [161]. The typical size range of the produced nanoparticles is 20–30 nm. The particle size can be varied by milling time and the heat treatment temperature. Physical vapor syntheses use the plasma arc energy intake by a solid precursor to generate a vapor at high temperature. Being decomposed into atoms, gases can react or condense to form particles when cooled [162].

Wet-chemical methods include hydrothermal/solvothermal processes, solution-liquid-solid, and surfactant-assisted synthesis. These methods provide a convenient and facile platform for a low-temperature fabrication of the desired ZnO nanostructures [163–165]. Typical precursors for ZnO nanocrystal preparation are zinc nitrate [166], metallic zinc [167], zinc chloride [168], zinc acetate [169, 170], and zinc sulfate [171]. If an anisotropic growth of ZnO nanoparticles is desired, surfactants such as hexamethylenetetramine [172], ammonia [173], ascorbic acid [174], and sodium hydroxide [175] can be added. Most reactions are performed at elevated temperatures up to 180 °C [165]. As shown in Fig. 1.9, different kinds of ZnO nanoparticles are obtained by adjusting the hydrolysis ratio. The nature of the protective agent added during ZnO formation and hydrolysis ratio are two major handles for size and shape control [176].

1.4.2 Titanium Dioxide Nanoparticles

Titanium dioxide nanoparticles are among the most frequently used metal oxide nanoparticles in industrial products and consumer goods [177]. Due to its very high refractive index and brightness, TiO_2 is extensively utilized as a white pigment with an annual consumption of almost four million tons worldwide [178]. Typical applications comprise paints [179, 180], coatings [181], plastics [182], papers [183], inks [184], pharmaceuticals [185], food products [186], cosmetics [187, 188], sun screens [189], and toothpaste [190]. Rompelberg et al. estimated the oral intake of TiO_2 from

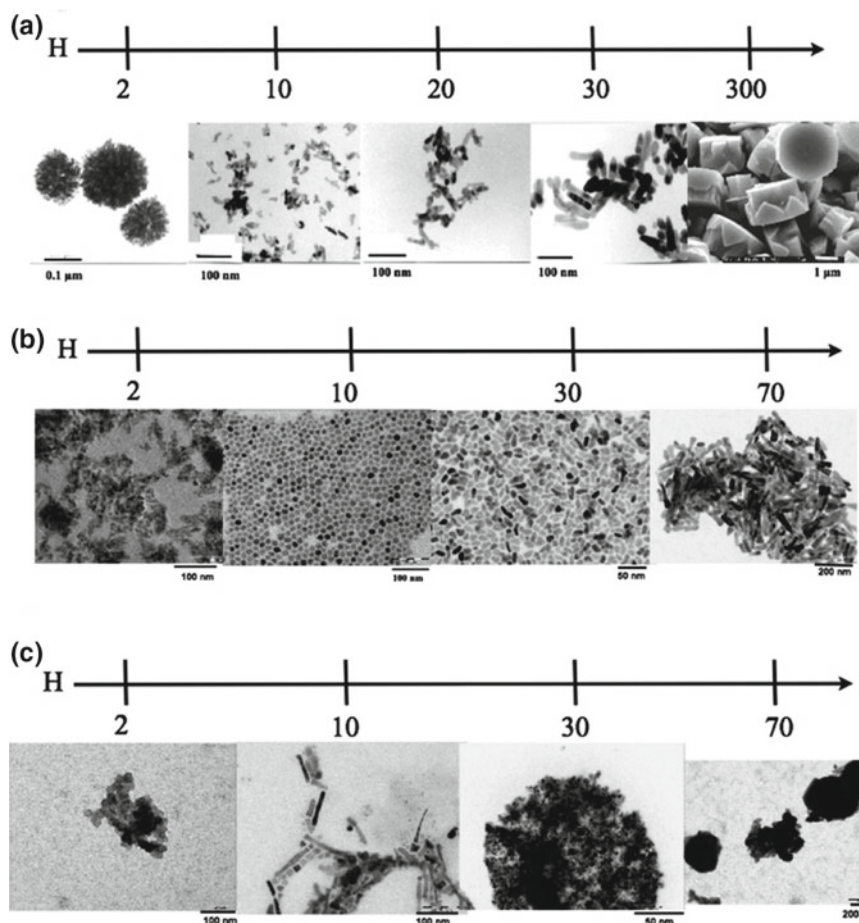


Fig. 1.9 TEM micrographs of ZnO nanoparticles synthesized in diethylene glycol (DEG) by variation of the hydrolysis ratio (H): **a** ZnO without addition of protective agents, **b** ZnO- tri-*n*-octylphosphine oxide, and **c** ZnO-polyoxyethylene stearyl ether. (Reproduced with permission from Langmuir 26, 9, 6522–6528. Copyright 2010 American Chemical Society) [176]

food, food supplements and toothpaste by measuring the total titanium concentrations and subsequently calculated the TiO_2 concentrations in selected representative Dutch food products (see Table 1.1) [186].

Several processes have been developed for the preparation of nanostructured TiO_2 with distinct characteristics. Commercial powders are typically prepared by the so-called chloride-process from TiCl_4 using hydrocarbon-assisted flame synthesis [191]. In the sulfate-process, ilmenite (FeTiO_3) is treated with concentrated sulfuric acid, and the titanium oxygen sulfate (TiOSO_4) is extracted and converted into titanium dioxide [192].

Table 1.1 Average measured total titanium concentrations and subsequently calculated TiO₂ concentrations in selected representative Dutch food products, raw (cow) milk, and food supplements. Samples rich in calcium were analyzed by ICP-HRMS, others by ICP-QMS. Limit of quantitation 0.05 mg Ti/kg product. (Reproduced from Rompelberg et al., 2016, *Nanotoxicology*, 10:10, 1404–1414 © 2016 National Institute for Public Health and the Environment. Published by Informa UK Limited, trading as Taylor & Francis Group) [187]

	Number of samples	Mean total-Ti (mg/kg product) (\pm SD)	Min total-Ti (mg/kg product)	Max total-Ti (mg/kg product)	Mean TiO ₂ (mg/kg product)
<i>Samples analysed by ICP-HRMS</i>					
Raw (cow) milk	6 (6)	0.31(\pm 0.23)	0.05	0.63	0.51
Regular dairy products (i.e. milk, yoghurt)	11 (10)	0.47(\pm 0.46)	<LOQ	1.46	0.79
Processed dairy products	10 (5)	0.12(\pm 0.17)	<LOQ	0.57	0.21
Soy milk	2 (2)	0.33(\pm 0.01)	0.32	0.34	0.55
Dutch cake with icing and cream	1 (1)	0.23	0.23	0.23	0.38
Coffee creamer (powdered)	1 (1)	1640	1640	1640	2739
<i>Samples analysed by ICP-QMS</i>					
Energy drink (containing caffeine)	1 (1)	0.07	0.07	0.07	0.11
Soft drink	2 (2)	0.06 (\pm 0.00)	0.06	0.07	0.11
Sports drink	2 (2)	0.09 (\pm 0.05)	0.05	0.12	0.14
Syrup	2 (2)	0.17 (\pm 0.00)	0.17	0.17	0.28
Ice (water-based)	1 (1)	0.16	0.16	0.16	0.26
Wine gums	1 (1)	0.25	0.25	0.25	0.42
Salad dressing	1 (1)	0.43	0.43	0.43	0.72
Food supplement (multivitamin)	2 (2)	744 (\pm 1009)	31	1458	1242

The wet-chemical fabrication of TiO_2 nanoparticles allows to control the stoichiometry, homogeneity, and morphology of the resulting materials. Nevertheless, the drawbacks are expensive precursors, long processing times, the nanoparticle isolation/purification after the synthesis, and the presence of impurities. The sol-gel technique is based on the hydrolysis of the precursors of the metal alkoxides ($\text{Ti}(\text{OR})_4$) with further thermal decomposition [193]. By controlling solution composition, pH, and temperature, the particle size can be tuned [194]. The precipitation process involves the addition of NaOH , NH_4OH , or urea to metal precursors (e.g., TiCl_4), followed by thermal treatment to crystallize the oxide [195]. The hydrothermal method can be started from metallic Ti, oxidized by H_2O_2 [196]. Nanocrystalline TiO_2 can be prepared by mechanical alloying from a metastable intermediate phase, i.e. $\text{TiO}(\text{OH})_2$ powder [197]. By in-flight oxidation of titanium nitride powder in an r.f. thermal plasma reactor, the formation of core-shell structured composites (with TiN cores and oxide shells) was realized [198].

1.4.3 Silica Nanoparticles

Silicon dioxide (SiO_2) nanoparticles are extensively used since the 1950s in numerous applications like additives for rubber (also in tires) and plastics [199–201], strengthening filler for concrete [202, 203], abrasives in toothpaste [204], thickeners in foods [205], and anti-caking agents in foods (E551) [206, 207]. Due its excellent biocompatibility, low toxicity, easy surface modification, and facile synthetic routes, silica nanoparticles are suitable for biological applications as grafting platform for imaging, detecting, drug loading, and site-specific targeting [208–210]. Their particle size, crystallinity, porosity, and shape can be accurately controlled, enabling a fine-tuning of silica nanoparticles for the intended application.

The large scale production of silica nanoparticles is performed by flame aerosol technology [211]. Developed by Kloepper [212], this fabrication method is based on the continuous flame pyrolysis of vaporized silicon tetrachloride (SiCl_4) [213]. The produced silica forms branched aggregates, with the primary amorphous particles in the size range from 5 to 50 nm [214]. The particle size and the particle size distribution can be modified varying the concentration of the reactants, the flame temperature, and the gas dwell time in the combustion [211].

Established in 1968, the Stöber method is a widely used sol-gel process for silica nanoparticle synthesis [215]. This reaction permits a controlled evolution of spherical silica particles of uniform size in the size range of 50 nm to 2 μm . Catalyzed by ammonia, it is based on the hydrolysis of alkyl silicates (e.g., tetraethoxysilane (TEOS)), and the subsequent condensation of silicic acid in alcoholic solutions. The control of the ratio of solvent to TEOS permits a fine control of particle size in the Stöber method [216]. As shown in Fig. 1.10, the diameter of the synthesized particle decreases as the ratio of solvent to TEOS is increased. The method can be modified for the incorporation of organic dyes and other nanosized materials [217].

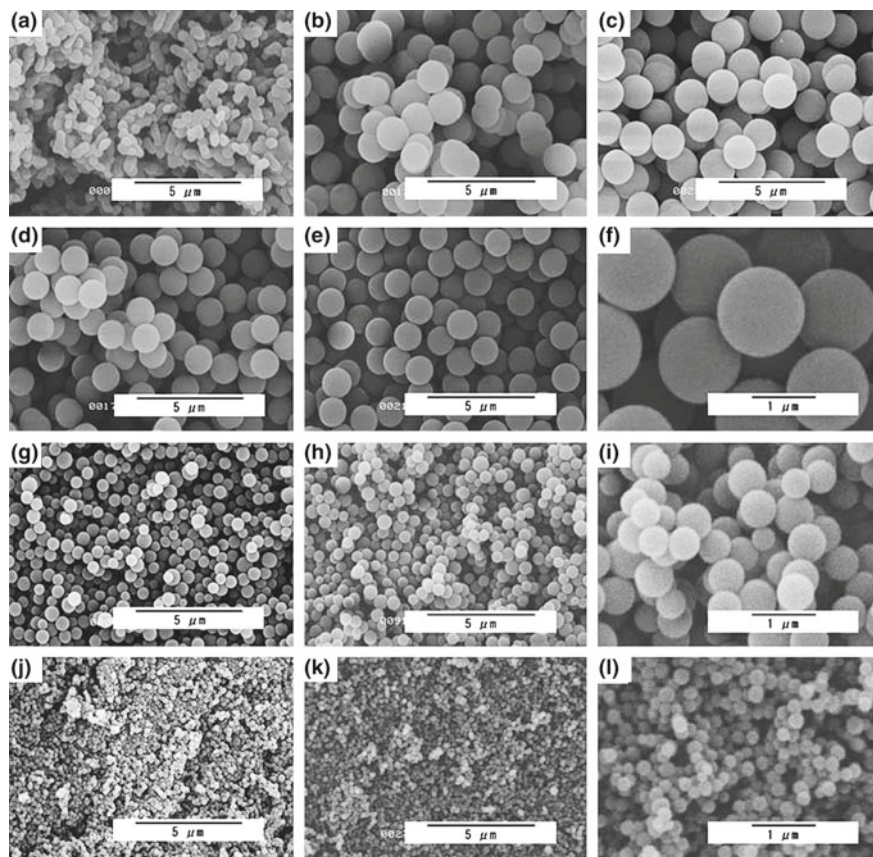


Fig. 1.10 Silica nanoparticles synthesized by the Stober method with variable methanol/TEOS ratios before and after calcination. The MeOH/TEOS synthesis ratios and calcined versus noncalcined status are as follows: **a** 300/noncalcined, **b** 750/noncalcined, **c** 1125/noncalcined, **d** 1500/noncalcined, **e** and **f** 1500/calcined, **g** 2250/noncalcined, **h** and **i** 2250/calcined, **j** 3000/noncalcined, and **k** and **l** 3000/calcined. As the ratio of methanol/TEOS increases from 300 to 1125, the particle size increases. However, from 1125 to 6000, the particle size decreased from 1500 to 10 nm in diameter [216]. (Reproduced with permission from Shimura, N. & Ogawa, M. *J Mater Sci* (2007) 42:5299 Copyright © 2007, Springer Nature)

Another important technique for silica nanoparticle preparation is the reverse microemulsion. Established by Arriagada and Osseo-Asare in the early 1990s, this method utilizes the ammonia-catalyzed polymerization of tetraethoxysilane in a reverse phase (water-in-oil microemulsion) [218]. The dispersion of nanodroplets leads to nanoreactors to form nanoparticles. The size of the colloids depends on the intrinsic properties of a surfactant and the molar ratio of water to surfactant [210]. The variation of the nanoparticle morphology can drastically affect their biodistribution, bioavailability, and toxicity [219, 220]. For instance, Trewyn et al. demonstrated the

effect of organic C_n-methylimidazolium ($n = 14, 16, 18$) derivatives on the modified Stöber synthesis [221]. The particles derived from modifications with C18MIM and C14OCMIM exhibited a rod- or worm-like structure.

References

1. Elghanian, R., et al.: Selective colorimetric detection of polynucleotides based on the distance-dependent optical properties of gold nanoparticles. *Science* **277**(5329), 1078 (1997)
2. Haes, A.J., Van Duyne, R.P.: A nanoscale optical biosensor: sensitivity and selectivity of an approach based on the localized surface plasmon resonance spectroscopy of triangular silver nanoparticles. *J. Am. Chem. Soc.* **124**(35), 10596–10604 (2002)
3. Sokolov, K., et al.: Real-time vital optical imaging of precancer using anti-epidermal growth factor receptor antibodies conjugated to gold nanoparticles. *Cancer Res.* **63**(9), 1999–2004 (2003)
4. El-Sayed, I.H., Huang, X., El-Sayed, M.A.: Surface plasmon resonance scattering and absorption of anti-EGFR antibody conjugated gold nanoparticles in cancer diagnostics: applications in oral cancer. *Nano Lett.* **5**(5), 829–834 (2005)
5. Alivisatos, P.: The use of nanocrystals in biological detection. *Nat. Biotechnol.* **22**, 47 (2003)
6. Li, Y.Y., et al.: Targeted polydopamine nanoparticles enable photoacoustic imaging guided chemo-photothermal synergistic therapy of tumor. *Acta Biomater.* **47**, 124–134 (2017)
7. Liu, J.N., Bu, W.B., Shi, J.L.: Chemical design and synthesis of functionalized probes for imaging and treating tumor hypoxia. *Chem. Rev.* **117**(9), 6160–6224 (2017)
8. Liu, G.L., et al.: Fluorescence enhancement of terminal amine assembled on gold nanoclusters and its application to ratiometric lysine detection. *Langmuir* **33**(51), 14643–14648 (2017)
9. Ricciardi, L., et al.: Plasmon-mediated cancer phototherapy: the combined effect of thermal and photodynamic processes. *Nanoscale* **9**(48), 19279–19289 (2017)
10. Chen, Y.P., Xianyu, Y.L., Jiang, X.Y.: Surface modification of gold nanoparticles with small molecules for biochemical analysis. *Acc. Chem. Res.* **50**(2), 310–319 (2017)
11. Xiang, Y., Lu, Y.: Using personal glucose meters and functional DNA sensors to quantify a variety of analytical targets. *Nat. Chem.* **3**(9), 697–703 (2011)
12. Hahn, M.A., et al.: Nanoparticles as contrast agents for in-vivo bioimaging: current status and future perspectives. *Anal. Bioanal. Chem.* **399**(1), 3–27 (2011)
13. Sailor, M.J., Park, J.H.: Hybrid nanoparticles for detection and treatment of cancer. *Adv. Mater.* **24**(28), 3779–3802 (2012)
14. Zhang, P.C., et al.: Recent progress in light-triggered nanotheranostics for cancer treatment. *Theranostics* **6**(7), 948–968 (2016)
15. Yang, Q.H., Xu, Q., Jiang, H.L.: Metal-organic frameworks meet metal nanoparticles: synergistic effect for enhanced catalysis. *Chem. Soc. Rev.* **46**(15), 4774–4808 (2017)
16. Jiang, K.Z., et al.: Efficient oxygen reduction catalysis by subnanometer Pt alloy nanowires. *Sci. Adv.* **3**(2), 8 (2017)
17. Eftekhari, A.: Electrocatalysts for hydrogen evolution reaction. *Int. J. Hydrogen Energy* **42**(16), 11053–11077 (2017)
18. Xu, H., et al.: Facile synthesis of Pd-Ru-P ternary nanoparticle networks with enhanced electrocatalytic performance for methanol oxidation. *Int. J. Hydrogen Energy* **42**(16), 11229–11238 (2017)
19. El-Sayed, M.A.: Some interesting properties of metals confined in time and nanometer space of different shapes. *Acc. Chem. Res.* **34**(4), 257–264 (2001)
20. Shenhar, R., Rotello, V.M.: Nanoparticles: scaffolds and building blocks. *Acc. Chem. Res.* **36**(7), 549–561 (2003)

21. Eustis, S., el-Sayed, M.A.: Why gold nanoparticles are more precious than pretty gold: noble metal surface plasmon resonance and its enhancement of the radiative and nonradiative properties of nanocrystals of different shapes. *Chem. Soc. Rev.* **35**(3), 209–217 (2006)
22. Toshima, N., Yonezawa, T.: Bimetallic nanoparticles—novel materials for chemical and physical applications. *New J. Chem.* **22**(11), 1179–1201 (1998)
23. Johnston, R.L.: *Atomic and Molecular Clusters*. Taylor & Francis (2002)
24. Sau, T.K., Rogach, A.L.: Nonspherical noble metal nanoparticles: colloid-chemical synthesis and morphology control. *Adv. Mater.* **22**(16), 1781–1804 (2010)
25. Sau, T.K., Murphy, C.J.: Room temperature, high-yield synthesis of multiple shapes of gold nanoparticles in aqueous solution. *J. Am. Chem. Soc.* **126**(28), 8648–8649 (2004)
26. Lee, H., et al.: Localized Pd overgrowth on cubic Pt nanocrystals for enhanced electrocatalytic oxidation of formic acid. *J. Am. Chem. Soc.* **130**(16), 5406–5407 (2008)
27. Zhang, J., et al.: Shape-selective synthesis of gold nanoparticles with controlled sizes, shapes, and plasmon resonances. *Adv. Funct. Mater.* **17**(16), 3295–3303 (2007)
28. Yu, Y.-T., Xu, B.-Q.: Shape-controlled synthesis of Pt nanocrystals: an evolution of the tetrahedral shape. *Appl. Organomet. Chem.* **20**(10), 638–647 (2006)
29. Schuetze, B., et al.: Conjugation of thiol-terminated molecules to ultrasmall 2 nm-gold nanoparticles leads to remarkably complex ¹H-NMR spectra. *J. Mater. Chem. B* **4**(12), 2179–2189 (2016)
30. Helmlinger, J., et al.: A rapid, high-yield and large-scale synthesis of uniform spherical silver nanoparticles by a microwave-assisted polyol process. *RSC Adv.* **5**(112), 92144–92150 (2015)
31. Sajanlal, P.R., Pradeep, T.: Electric-field-assisted growth of highly uniform and oriented gold nanotriangles on conducting glass substrates. *Adv. Mater.* **20**(5), 980–983 (2008)
32. Wang, L., et al.: Synthesis of gold nano- and microplates in hexagonal liquid crystals. *J. Phys. Chem. B* **109**(8), 3189–3194 (2005)
33. Djalali, R., Chen, Y.F., Matsui, H.: Au nanowire fabrication from sequenced histidine-rich peptide. *J. Am. Chem. Soc.* **124**(46), 13660–13661 (2002)
34. Faraday, M.: *X. The Bakerian Lecture. —Experimental relations of gold (and other metals) to light*. *Philos. Trans. R. Soc. Lond.* **147**, 145–181 (1857)
35. Turkevich, J., Stevenson, P.C., Hillier, J.: A study of the nucleation and growth processes in the synthesis of colloidal gold. *Discuss. Faraday Soc.* **11**, 55–75 (1951)
36. Frens, G.: Particle size and sol stability in metal colloids. *Kolloid-Zeitschrift und Zeitschrift für Polymere* **250**(7), 736–741 (1972)
37. Frens, G.: Controlled nucleation for the regulation of the particle size in monodisperse gold suspensions. *NPhS* **241**, 20 (1973)
38. Huang, X., et al.: One-step, size-controlled synthesis of gold nanoparticles at room temperature using plant tannin. *Green Chem.* **12**(3), 395–399 (2010)
39. Mahl, D., et al.: Silver, gold, and alloyed silver–gold nanoparticles: characterization and comparative cell-biologic action. *J. Nanopart. Res.* **14**(10), 1153 (2012)
40. Shang, L., et al.: One-pot synthesis of near-infrared fluorescent gold clusters for cellular fluorescence lifetime imaging. *Small* **7**(18), 2614–2620 (2011)
41. Jana, N.R., Gearheart, L., Murphy, C.J.: Seeding growth for size control of 5–40 nm diameter gold nanoparticles. *Langmuir* **17**(22), 6782–6786 (2001)
42. Perrault, S.D., Chan, W.C.W.: Synthesis and surface modification of highly monodispersed, spherical gold nanoparticles of 50–200 nm. *J. Am. Chem. Soc.* **131**(47), 17042–17043 (2009)
43. Ristig, S., et al.: An easy synthesis of autofluorescent alloyed silver-gold nanoparticles. *J. Mater. Chem. B* **2**(45), 7887–7895 (2014)
44. Brust, M., et al.: Synthesis of thiol-derivatised gold nanoparticles in a two-phase liquid-liquid system. *J. Chem. Soc. Chem. Commun.* **7**, 801–802 (1994)
45. Allpress, J.G., Sanders, J.V.: The structure and orientation of crystals in deposits of metals on mica. *Surf. Sci.* **7**(1), 1–25 (1967)
46. Structural studies of trigonal lamellar particles of gold and silver. *Proc. R. Soc. Lond. Ser. A: Math. Phys. Sci.* **440**(1910), 589–609 (1993)

47. Sun, Y., Xia, Y.: Shape-controlled synthesis of gold and silver nanoparticles. *Science* **298**(5601), 2176 (2002)
48. Rehbock, C., et al.: Size control of laser-fabricated surfactant-free gold nanoparticles with highly diluted electrolytes and their subsequent bioconjugation. *PCCP* **15**(9), 3057–3067 (2013)
49. Semaltianos, N.G.: Nanoparticles by laser ablation. *Crit. Rev. Solid State Mater. Sci.* **35**(2), 105–124 (2010)
50. Popovic, D.M., et al.: Continuous wave laser for tailoring the photoluminescence of silicon nanoparticles produced by laser ablation in liquid. *J. Appl. Phys.* **122**(11), 113107 (2017)
51. Tsuji, T., et al.: Preparation of silver nanoparticles by laser ablation in solution: influence of laser wavelength on particle size. *Appl. Surf. Sci.* **202**(1), 80–85 (2002)
52. Walter, J.G., et al.: Laser ablation-based one-step generation and bio-functionalization of gold nanoparticles conjugated with aptamers. *J. Nanobiotechnol.* **8**(1), 21 (2010)
53. Jin, R., et al.: Atomically precise colloidal metal nanoclusters and nanoparticles: fundamentals and opportunities. *Chem. Rev.* **116**(18), 10346–10413 (2016)
54. Schmid, G.: The relevance of shape and size of Au₅₅ clusters. *Chem. Soc. Rev.* **37**(9), 1909–1930 (2008)
55. Hakkinen, H.: Atomic and electronic structure of gold clusters: understanding flakes, cages and superatoms from simple concepts. *Chem. Soc. Rev.* **37**(9), 1847–1859 (2008)
56. Schmid, G., et al.: Au₅₅[P(C₆H₅)₃]₁₂Cl₆—ein Goldcluster ungewöhnlicher Größe. *Chem. Ber.* **114**(11), 3634–3642 (1981)
57. Newton, M.G., et al.: Symmetrical and unsymmetrical bridging carbonyl groups in binuclear molybdenum carbonyl complexes of alkylaminobis(difluorophosphines); X-ray crystal structures of two of the complexes. *J. Chem. Soc. Chem. Commun.* (3), 201–203 (1982)
58. Tyo, E.C., Vajda, S.: Catalysis by clusters with precise numbers of atoms. *Nat. Nanotechnol.* **10**, 577 (2015)
59. Nonappa, et al., Template-free supracolloidal self-assembly of atomically precise gold nanoclusters: from 2D Colloidal crystals to spherical capsids. *Angew. Chem. Int. Ed.* **55**(52), 16035–16038 (2016)
60. Mahl, D.: *Synthese, Löslichkeit und Stabilität von Gold-Nanopartikeln in biologischen Medien.* University of Duisburg-Essen, Essen (2011)
61. Nowack, B., Krug, H.F., Height, M.: 120 years of nanosilver history: implications for policy makers. *Environ. Sci. Technol.* **45**(4), 1177–1183 (2011)
62. Xu, H., Suslick, K.S.: Sonochemical synthesis of highly fluorescent Ag nanoclusters. *ACS Nano* **4**(6), 3209–3214 (2010)
63. Chen, J., et al.: A simple and versatile mini-arc plasma source for nanocrystal synthesis. *J. Nanopart. Res.* **9**(2), 203–213 (2007)
64. Wägener, P., et al.: Dynamics of silver nanoparticle formation and agglomeration inside the cavitation bubble after pulsed laser ablation in liquid. *PCCP* **15**(9), 3068–3074 (2013)
65. Lea, M.C.: Allotropic forms of silver. *Am. J. Sci. (Series 3)* **37**(222), 476–491 (1889)
66. Kittler, S., et al.: Toxicity of silver nanoparticles increases during storage because of slow dissolution under release of silver ions. *Chem. Mater.* **22**(16), 4548–4554 (2010)
67. Banerjee, S., et al.: Structural evolution of silver nanoparticles during wet-chemical synthesis. *Chem. Mater.* **26**(2), 951–957 (2014)
68. Firdhouse, M.J., Lalitha, P.: Biosynthesis of silver nanoparticles and its applications. *J. Nanotechnol.* **2015**, 18 (2015)
69. Prabhu, S., Poulouse, E.K.: Silver nanoparticles: mechanism of antimicrobial action, synthesis, medical applications, and toxicity effects. *Int. Nano Lett.* **2**(1), 32 (2012)
70. Mavani, K., Shah, M.: Synthesis of silver nanoparticles by using sodium borohydride as a reducing agent (2013)
71. Kim, D., Jeong, S., Moon, J.: Synthesis of silver nanoparticles using the polyol process and the influence of precursor injection. *Nanotechnology* **17**(16), 4019–4024 (2006)
72. Zhao, T., et al.: Size-controlled preparation of silver nanoparticles by a modified polyol method. *Colloid Surf A: Physicochem. Eng. Aspects* **366**(1), 197–202 (2010)

73. Won, H., et al.: Preparation of porous silver particles using ammonium formate and its formation mechanism. *Chem. Eng. J.* **156**, 459–464 (2010)
74. Chen, S., Fan, Z., Carroll, D.L.: Silver nanodisks: synthesis, characterization, and self-assembly. *J. Phys. Chem. B* **106**(42), 10777–10781 (2002)
75. Rycenga, M., McLellan, J.M., Xia, Y.: Controlling the assembly of silver nanocubes through selective functionalization of their faces. *Adv. Mater.* **20**(12), 2416–2420 (2008)
76. Schuette, W.M., Buhro, W.E.: Silver chloride as a heterogeneous nucleant for the growth of silver nanowires. *ACS Nano* **7**(5), 3844–3853 (2013)
77. Zinchenko, A.A., Yoshikawa, K., Baigl, D.: DNA-templated silver nanorings. *Adv. Mater.* **17**(23), 2820–2823 (2005)
78. Wiley, B.J., et al.: Right bipyramids of silver: a new shape derived from single twinned seeds. *Nano Lett.* **6**(4), 765–768 (2006)
79. Im, S.H., et al.: Large-scale synthesis of silver nanocubes: the role of hcl in promoting cube perfection and monodispersity. *Angew. Chem. Int. Ed.* **44**(14), 2154–2157 (2005)
80. Darmanin, T., et al.: Microwave-assisted synthesis of silver nanoprisms/nanoplates using a “modified polyol process”. *Colloids Surf. Physicochem. Eng. Aspects* **395**, 145–151 (2012)
81. Helmlinger, J., et al.: On the crystallography of silver nanoparticles with different shapes. *Cryst. Growth Des.* **16**(7), 3677–3687 (2016)
82. Wiley, B., et al.: Shape-controlled synthesis of metal nanostructures: the case of silver. *Chem. – A Eur. J.* **11**(2), 454–463 (2005)
83. Ye, X., et al.: Morphologically controlled synthesis of colloidal upconversion nanophosphors and their shape-directed self-assembly. *Proc. Natl. Acad. Sci. USA* **107**(52), 22430–22435 (2010)
84. Bratlie, K.M., et al.: Platinum nanoparticle shape effects on benzene hydrogenation selectivity. *Nano Lett.* **7**(10), 3097–3101 (2007)
85. Tian, N., et al.: Synthesis of tetrahedral platinum nanocrystals with high-index facets and high electro-oxidation activity. *Science* **316**(5825), 732–735 (2007)
86. Roldan Cuenya, B.: Metal nanoparticle catalysts beginning to shape-up. *Acc. Chem. Res.* **46**(8), 1682–1691 (2013)
87. Schmid, G.: Large clusters and colloids. Metals in the embryonic state. *Chem. Rev.* **92**(8), 1709–1727 (1992)
88. Song, H., et al.: Pt nanocrystals: shape control and langmuir–blodgett monolayer formation. *J. Phys. Chem. B* **109**(1), 188–193 (2005)
89. Kang, Y., et al.: Shape-controlled synthesis of Pt nanocrystals: the role of metal carbonyls. *ACS Nano* **7**(1), 645–653 (2013)
90. Henglein, A., Ershov, B.G., Malow, M.: Absorption spectrum and some chemical reactions of colloidal platinum in aqueous solution. *J. Phys. Chem.* **99**(38), 14129–14136 (1995)
91. Kang, Y., Ye, X., Murray, C.B.: Size- and shape-selective synthesis of metal nanocrystals and nanowires using CO as a reducing agent. *Angew. Chem. Int. Ed. Engl.* **49**(35), 6156–6159 (2010)
92. Zhao, S.-Y., et al.: Preparation, phase transfer, and self-assembled monolayers of cubic Pt nanoparticles. *Langmuir* **18**(8), 3315–3318 (2002)
93. Lee, S.-A., et al.: Nanoparticle synthesis and electrocatalytic activity of Pt alloys for direct methanol fuel cells. *J. Electrochem. Soc.* **149**(10), A1299–A1304 (2002)
94. Liu, Z., et al.: Nanosized Pt and PtRu colloids as precursors for direct methanol fuel cell catalysts. *J. Mater. Chem.* **13**(12), 3049–3052 (2003)
95. Herricks, T., Chen, J., Xia, Y.: Polyol synthesis of platinum nanoparticles: control of morphology with sodium nitrate. *Nano Lett.* **4**(12), 2367–2371 (2004)
96. Fujimoto, T., et al.: Sonochemical preparation of single-dispersion metal nanoparticles from metal salts. *Chem. Mater.* **13**(3), 1057–1060 (2001)
97. Falicov, L.M., Somorjai, G.A.: Correlation between catalytic activity and bonding and coordination number of atoms and molecules on transition metal surfaces: theory and experimental evidence. *Proc. Natl. Acad. Sci. USA* **82**(8), 2207–2211 (1985)

98. Wang, C., et al.: A general approach to the size- and shape-controlled synthesis of platinum nanoparticles and their catalytic reduction of oxygen. *Angew. Chem. Int. Ed.* **47**(19), 3588–3591 (2008)
99. Teng, X., Yang, H.: Synthesis of platinum multipods: an induced anisotropic growth. *Nano Lett.* **5**(5), 885–891 (2005)
100. Chen, J., et al.: Single-crystal nanowires of platinum can be synthesized by controlling the reaction rate of a polyol process. *J. Am. Chem. Soc.* **126**(35), 10854–10855 (2004)
101. Barcikowski, S., Compagnini, G.: Advanced nanoparticle generation and excitation by lasers in liquids. *PCCP* **15**(9), 3022–3026 (2013)
102. Angelov, S.D., et al.: Electrophoretic deposition of ligand-free platinum nanoparticles on neural electrodes affects their impedance in vitro and in vivo with no negative effect on reactive gliosis. *J. Nanobiotechnology* **14**(1), 3 (2016)
103. Khan, F.A.: *Biotechnology Fundamentals*. CRC Press, Boca Raton (2011)
104. Seku, K., et al.: Hydrothermal synthesis of Copper nanoparticles, characterization and their biological applications. *Int. J. Nano Dimens.* **9**(1), 7–14 (2018)
105. Sanchez-Sanhueza, G., et al.: Synthesis of Copper nanowires and their antimicrobial activity on strains isolated persistent endodontic infections. *J. Nanosci. Nanotechnol.* **18**(7), 4507–4514 (2018)
106. Shabnam, L., et al.: Doped graphene/Cu nanocomposite: a high sensitivity non-enzymatic glucose sensor for food. *Food Chem.* **221**, 751–759 (2017)
107. Lee, Y., et al.: Large-scale synthesis of Copper nanoparticles by chemically controlled reduction for applications of inkjet-printed electronics. *Nanotechnology* **19**(41), 415604 (2008)
108. Ranu, B.C., et al.: Copper nanoparticle-catalyzed carbon-carbon and carbon-heteroatom bond formation with a greener perspective. *ChemSusChem* **5**(1), 22–44 (2012)
109. Allen, S.E., et al.: Aerobic copper-catalyzed organic reactions. *Chem. Rev.* **113**(8), 6234–6458 (2013)
110. Kaur, R., Pal, B.: Cu nanostructures of various shapes and sizes as superior catalysts for nitroaromatic reduction and co-catalyst for Cu/TiO₂ photocatalysis. *Appl. Catal. A* **491**, 28–36 (2015)
111. Parveen, F., et al.: Copper nanoparticles: synthesis methods and its light harvesting performance. *Sol. Energy Mater. Sol. Cells* **144**, 371–382 (2016)
112. Tilaki, R.M., Irajizad, A., Mahdavi, S.M.: Size, composition and optical properties of copper nanoparticles prepared by laser ablation in liquids. *Appl. Phys. A* **88**(2), 415–419 (2007)
113. Salavati-Niasari, M., Fereshteh, Z., Davar, F.: Synthesis of oleylamine capped copper nanocrystals via thermal reduction of a new precursor. *Polyhedron* **28**(1), 126–130 (2009)
114. Park, B.K., et al.: Direct writing of copper conductive patterns by ink-jet printing. *Thin Solid Films* **515**(19), 7706–7711 (2007)
115. Woo, K., et al.: Ink-jet printing of Cu-Ag-based highly conductive tracks on a transparent substrate. *Langmuir* **25**(1), 429–433 (2009)
116. Khan, A., et al.: A chemical reduction approach to the synthesis of copper nanoparticles. *Int. Nano Lett.* **6**(1), 21–26 (2016)
117. Gawande, M.B., et al.: Cu and Cu-based nanoparticles: synthesis and applications in catalysis. *Chem. Rev.* **116**(6), 3722–3811 (2016)
118. Wu, C., Mosher, B.P., Zeng, T.: One-step green route to narrowly dispersed copper nanocrystals. *J. Nanopart. Res.* **8**(6), 965–969 (2006)
119. Thi My Dung, D., et al.: Synthesis and optical properties of copper nanoparticles prepared by a chemical reduction method. *Adv. Nat. Sci.: Nanosci. Nanotechnol.* **2**(1), 015009 (2011)
120. Chernogorenko, V.B., Tasybaeva, S.T.: Mechanism of chemical, reduction of copper(II) by hypophosphite ion. *Russ. J. Appl. Chem.* **68**(4), 461–464 (1995)
121. Jeong, S., et al.: Controlling the thickness of the surface oxide layer on Cu nanoparticles for the fabrication of conductive structures by Ink-jet printing. *Adv. Funct. Mater.* **18**(5), 679–686 (2008)
122. Wei, Y., et al.: Synthesis of stable, low-dispersity copper nanoparticles and nanorods and their antifungal and catalytic properties. *J. Phys. Chem. C* **114**(37), 15612–15616 (2010)

123. Ferrando, R., Jellinek, J., Johnston, R.L.: Nanoalloys: from theory to applications of alloy clusters and nanoparticles. *Chem. Rev.* **108**(3), 845–910 (2008)
124. Wanjala, B.N., et al.: Nanoscale alloying, phase-segregation, and core–shell evolution of gold–platinum nanoparticles and their electrocatalytic effect on oxygen reduction reaction. *Chem. Mater.* **22**(14), 4282–4294 (2010)
125. Tahir, M., Tahir, B., Amin, N.A.S.: Synergistic effect in plasmonic Au/Ag alloy NPs co-coated TiO₂ NWs toward visible-light enhanced CO₂ photoreduction to fuels. *Appl. Catal. B* **204**, 548–560 (2017)
126. Bennett, E., et al.: A synthetic route for the effective preparation of metal alloy nanoparticles and their use as active electrocatalysts. *ACS Catal.* **6**(3), 1533–1539 (2016)
127. Ristig, S., et al.: Synthesis, characterization and in vitro effects of 7 nm alloyed silver–gold nanoparticles. *Beilstein J. Nanotechnol.* **6**, 1212–1220 (2015)
128. Taylor, U., et al.: Influence of gold, silver and gold–silver alloy nanoparticles on germ cell function and embryo development. *Beilstein J. Nanotechnol.* **6**, 651–664 (2015)
129. Ruban, A.V., Skriver, H.L., Nørskov, J.K.: Surface segregation energies in transition-metal alloys. *PhRvB* **59**(24), 15990–16000 (1999)
130. Molenbroek, A.M., Haukka, S., Clausen, B.S.: Alloying in Cu/Pd Nanoparticle Catalysts. *J. Phys. Chem. B* **102**(52), 10680–10689 (1998)
131. Nanosized clusters on and in supports—perspectives for future catalysis, in metal clusters in chemistry
132. Andrews, M.P., O’Brien, S.C.: Gas-phase “molecular alloys” of bulk immiscible elements: iron-silver (FeAg). *J. Phys. Chem.* **96**(21), 8233–8241 (1992)
133. Cortie, M.B., McDonagh, A.M.: Synthesis and optical properties of hybrid and alloy plasmonic nanoparticles. *Chem. Rev.* **111**(6), 3713–3735 (2011)
134. Zhang, D., Gökce, B., Barcikowski, S.: Laser synthesis and processing of colloids: fundamentals and applications. *Chem. Rev.* **117**(5), 3990–4103 (2017)
135. Simakin, A.V., et al.: Nanoparticles produced by laser ablation of solids in liquid environment. *Appl. Phys. A* **79**(4), 1127–1132 (2004)
136. Tiedemann, D., et al.: Reprotoxicity of gold, silver, and gold-silver alloy nanoparticles on mammalian gametes. *Analyst* **139**(5), 931–942 (2014)
137. Goia, D.V., Matijevic, E.: Preparation of monodispersed metal particles. *New J. Chem.* **22**(11), 1203–1215 (1998)
138. Reetz, M.T., Helbig, W.: Size-selective synthesis of nanostructured transition metal clusters. *J. Am. Chem. Soc.* **116**(16), 7401–7402 (1994)
139. Tan, C., et al.: A self-supporting bimetallic Au@Pt core-shell nanoparticle electrocatalyst for the synergistic enhancement of methanol oxidation. *Sci. Rep.* **7**, 6347 (2017)
140. Rostek, A., Breisch, M., Loza, K., Garcia, P.R.A.F., Oliveira, C.L.P., Prymak, O., Heggen, M., Köller, M., Sengstock, C., Epple, M.: *ChemistrySelect* **3**, 4994 (2018)
141. Schlücker, S.: Surface-enhanced raman spectroscopy: concepts and chemical applications. *Angew. Chem. Int. Ed.* **53**(19), 4756–4795 (2014)
142. Rodríguez-Gonzalez, B., et al.: Multishell bimetallic AuAg nanoparticles: synthesis, structure and optical properties. *J. Mater. Chem.* **15**(17), 1755–1759 (2005)
143. Lintz, H.G., Kung, H.H.: *Transition Metal Oxides: Surface Chemistry and Catalysis*, Vol. 45, Studies in Surface Science and Catalysis, Elsevier, Amsterdam, Oxford, New York, Tokyo (1989)
144. Fernández-García, J.A.R.: *Synthesis, Properties, and Applications of Oxide Nanomaterials*. Wiley, New York (2006)
145. Miller, D.R., Akbar, S.A., Morris, P.A.: Nanoscale metal oxide-based heterojunctions for gas sensing: a review. *Sensors Actuators B: Chem.* **204**, 250–272 (2014)
146. Cui, T.H., Hua, F., Lvov, Y.: FET fabricated by layer-by-layer nanoassembly. *IEEE Trans. Electron Devices* **51**(3), 503–506 (2004)
147. Jeong, S.J., et al.: Characteristics of piezoelectric multilayer devices containing metal-oxide multicomponent electrode. *Ferroelectrics* **338**, 425- + (2006)

148. Winter, M., Brodd, R.J.: What are batteries, fuel cells, and supercapacitors? *Chem. Rev.* **104**(10), 4245–4270 (2004)
149. Hu, J.S., et al.: Synthesis of hierarchically structured metal oxides and their application in heavy metal ion removal. *Adv. Mater.* **20**(15), 2977–2982 (2008)
150. Wang, F.Y., et al.: Manipulating III–V nanowire transistor performance via surface decoration of metal-oxide nanoparticles. *Adv. Mater. Interfaces* **4**(12), 1700260 (2017)
151. Kumar, K.Y., et al.: Low-cost synthesis of metal oxide nanoparticles and their application in adsorption of commercial dye and heavy metal ion in aqueous solution. *Powder Technol.* **246**, 125–136 (2013)
152. Stoimenov, P.K., et al.: Metal oxide nanoparticles as bactericidal agents. *Langmuir* **18**(17), 6679–6686 (2002)
153. Serpone, N., Dondi, D., Albini, A.: Inorganic and organic UV filters: their role and efficacy in sunscreens and sun care product. *Inorg. Chim. Acta* **360**(3), 794–802 (2007)
154. Wang, H.T., et al.: Bifunctional non-noble metal oxide nanoparticle electrocatalysts through lithium-induced conversion for overall water splitting. *Nat. Commun.* **6**, 7261 (2015)
155. Wang, Z.L.: Zinc oxide nanostructures: growth, properties and applications. *J. Phys.: Condens. Matter* **16**(25), R829 (2004)
156. Moezzi, A., McDonagh, A.M., Cortie, M.B.: Zinc oxide particles: synthesis, properties and applications. *Chem. Eng. J.* **185–186**, 1–22 (2012)
157. Frederickson, C.J., Koh, J.-Y., Bush, A.I.: The neurobiology of zinc in health and disease. *Nat. Rev. Neurosci.* **6**, 449 (2005)
158. Code of Federal Regulations Title 21 (2017). <https://www.accessdata.fda.gov/scripts/cdrh/cfdocs/cfcfr/CFRSearch.cfm?fr=182.8991>
159. Espitia, P.J.P., et al.: Zinc oxide nanoparticles: synthesis, antimicrobial activity and food packaging applications. *Food Bioprocess Technol.* **5**(5), 1447–1464 (2012)
160. Casey, P.: 1—Nanoparticle technologies and applications. In: *Nanostructure Control of Materials*, pp. 1–31. Woodhead Publishing (2006)
161. Aghababazadeh, R., et al.: ZnO nanoparticles synthesised by mechanochemical processing. *J. Phys: Conf. Ser.* **26**(1), 312 (2006)
162. Swihart, M.T.: Vapor-phase synthesis of nanoparticles. *Curr. Opin. Colloid Interface Sci.* **8**(1), 127–133 (2003)
163. Willander, M., et al.: ZnO nanowires: chemical growth, electrodeposition, and application to intracellular nano-sensors. *Phys. Status Solidi C* **5**(9), 3076–3083 (2008)
164. Hu, H., Deng, C., Huang, X.: Hydrothermal growth of center-hollow multigonal star-shaped ZnO architectures assembled by hexagonal conic nanotubes. *Mater. Chem. Phys.* **121**(1), 364–369 (2010)
165. Arya, S.K., et al.: Recent advances in ZnO nanostructures and thin films for biosensor applications: review. *Anal. Chim. Acta* **737**, 1–21 (2012)
166. Zhao, J., Wu, L., Zhi, J.: Fabrication of micropatterned ZnO/SiO₂ core/shell nanorod arrays on a nanocrystalline diamond film and their application to DNA hybridization detection. *J. Mater. Chem.* **18**(21), 2459–2465 (2008)
167. Zeng, H., et al.: Microstructure control of Zn/ZnO core/shell nanoparticles and their temperature-dependent blue emissions. *J. Phys. Chem. B* **111**(51), 14311–14317 (2007)
168. Wei, A., et al.: Enzymatic glucose biosensor based on ZnO nanorod array grown by hydrothermal decomposition. *Appl. Phys. Lett.* **89**(12), 123902 (2006)
169. Yu, L., Qu, F., Wu, X.: Solution synthesis and optimization of ZnO nanowindmills. *Appl. Surf. Sci.* **257**(17), 7432–7435 (2011)
170. Daumann, S., et al.: Water-free synthesis of ZnO quantum dots for application as an electron injection layer in light-emitting electrochemical cells. *J. Mater. Chem. C* **5**(9), 2344–2351 (2017)
171. Dai, Z., et al.: Immobilization and direct electrochemistry of glucose oxidase on a tetragonal pyramid-shaped porous ZnO nanostructure for a glucose biosensor. *Biosens. Bioelectron.* **24**(5), 1286–1291 (2009)

172. Lei, Y., et al.: Improved glucose electrochemical biosensor by appropriate immobilization of nano-ZnO. *Colloids Surf. B. Biointerfaces* **82**(1), 168–172 (2011)
173. Liu, J., et al.: Vertically aligned 1D ZnO nanostructures on bulk alloy substrates: direct solution synthesis, photoluminescence, and field emission. *J. Phys. Chem. C* **111**(13), 4990–4997 (2007)
174. Xia, C., et al.: Synthesis of nanochain-assembled ZnO flowers and their application to dopamine sensing. *Sensors Actuators B: Chem.* **147**(2), 629–634 (2010)
175. Zhang, Y., et al.: An enzyme immobilization platform for biosensor designs of direct electrochemistry using flower-like ZnO crystals and nano-sized gold particles. *J. Electroanal. Chem.* **627**(1), 9–14 (2009)
176. Brayner, R., et al.: ZnO nanoparticles: synthesis, characterization, and ecotoxicological studies. *Langmuir* **26**(9), 6522–6528 (2010)
177. Shukla, R.K., et al.: ROS-mediated genotoxicity induced by titanium dioxide nanoparticles in human epidermal cells. *Toxicol. In Vitro* **25**(1), 231–241 (2011)
178. Ortlieb, M.: White giant or white dwarf?: particle size distribution measurements of TiO₂. *GIT Lab. J. Eur.* **14**, 42–43 (2010)
179. Taheri, M., Jahanfar, M., Ogino, K.: Self-cleaning traffic marking paint. *Surf. Interfaces* **9**, 13–20 (2017)
180. Fadhilah, N., et al.: Self-cleaning limestone paint modified by nanoparticles TiO₂ synthesized from TiCl₃ as precursors and PEG6000 as dispersant. *Bull. Chem. React. Eng. Catal.* **12**(3), 351–356 (2017)
181. Du, Z.F., et al.: Enhanced photocatalytic activity of Bi₂WO₆/TiO₂ composite coated polyester fabric under visible light irradiation. *Appl. Surf. Sci.* **435**, 626–634 (2018)
182. Olariu, M.A., et al.: Electrical properties of polyimide composite films containing TiO₂ nanotubes. *Polym. Compos.* **38**(11), 2584–2593 (2017)
183. Xu, W.J., et al.: Superhydrophobic titania nanoparticles for fabrication of paper-based analytical devices: an example of heavy metals assays. *Talanta* **181**, 333–339 (2018)
184. Imran, M., et al.: Oxygen-deficient TiO(2-x)methylene blue colloids: highly efficient photoreversible intelligent ink. *Langmuir* **32**(35), 8980–8987 (2016)
185. Ruiz, P.A., et al.: Titanium dioxide nanoparticles exacerbate DSS-induced colitis: role of the NLRP3 inflammasome. *Gut* **66**(7), 1216–1224 (2017)
186. Rompelberg, C., et al.: Oral intake of added titanium dioxide and its nanofraction from food products, food supplements and toothpaste by the Dutch population. *Nanotoxicology* **10**(10), 1404–1414 (2016)
187. Choi, S., et al.: A seasonal observation on the distribution of engineered nanoparticles in municipal wastewater treatment systems exemplified by TiO₂ and ZnO. *Sci. Total Environ.* **625**, 1321–1329 (2018)
188. Nohynek, G.J., et al.: Grey goo on the skin? Nanotechnology, cosmetic and sunscreen safety. *Crit. Rev. Toxicol.* **37**(3), 251–277 (2007)
189. Lewicka, Z.A., et al.: Photochemical behavior of nanoscale TiO₂ and ZnO sunscreen ingredients. *Journal of Photochemistry and Photobiology a-Chemistry* **263**, 24–33 (2013)
190. de la Calle, I., et al.: Screening of TiO₂ and Au nanoparticles in cosmetics and determination of elemental impurities by multiple techniques (DLS, SP-ICP-MS, ICP-MS and ICP-OES). *Talanta* **171**, 291–306 (2017)
191. Titanium Compounds, Inorganic, in Kirk-Othmer Encyclopedia of Chemical Technology
192. Góñezquez, M.J.s., et al.: A review of the production cycle of titanium dioxide pigment. *Mater. Sci. Appl.* **05**(07), 18 (2014)
193. Behnajady, M.A., et al.: Investigation of the effect of sol-gel synthesis variables on structural and photocatalytic properties of TiO₂ nanoparticles. *Desalination* **278**(1), 10–17 (2011)
194. Burda, C., et al.: Chemistry and properties of nanocrystals of different shapes. *Chem. Rev.* **105**(4), 1025–1102 (2005)
195. Carp, O., Huisman, C.L., Reller, A.: Photoinduced reactivity of titanium dioxide. *Prog. Solid State Chem.* **32**(1), 33–177 (2004)

196. Qian, Y., et al.: Preparation of ultrafine powders of TiO₂ by hydrothermal H₂O₂ oxidation starting from metallic Ti. *J. Mater. Chem.* **3**(2), 203–205 (1993)
197. Kim, D.H., et al.: Photocatalytic behaviors and structural characterization of nanocrystalline Fe-doped TiO₂ synthesized by mechanical alloying. *J. Alloys Compd.* **375**(1), 259–264 (2004)
198. Oh, S.-M., Ishigaki, T.: Preparation of pure rutile and anatase TiO₂ nanopowders using RF thermal plasma. *Thin Solid Films* **457**(1), 186–191 (2004)
199. Susanna, A., et al.: Catalytic effect of ZnO anchored silica nanoparticles on rubber vulcanization and cross-link formation. *Eur. Polym. J.* **93**, 63–74 (2017)
200. Liu, Z.J., Zhang, Y.: Enhanced mechanical and thermal properties of SBR composites by introducing graphene oxide nanosheets decorated with silica particles. *Compos. Part A-Appl. Sci. Manuf.* **102**, 236–242 (2017)
201. Zhao, X.L., et al.: Surface modification of ultra-high molecular weight polyethylene fiber by different kinds of SiO₂ nanoparticles. *Polym. Compos.* **38**(9), 1928–1936 (2017)
202. Mosquera, M.J., Carrascosa, L.A.M., Badreldin, N.: Producing superhydrophobic/oleophobic coatings on cultural heritage building materials. *Pure Appl. Chem.* **90**(3), 551–561 (2018)
203. Bernal, J., et al.: Fresh and mechanical behavior of a self-compacting concrete with additions of nano-silica, silica fume and ternary mixtures. *Constr. Build. Mater.* **160**, 196–210 (2018)
204. Willknitz, P.: Cleaning power and abrasivity of European toothpastes. *Adv. Dental Res.* **11**(4), 576–579 (1997)
205. Younes, M., et al.: Re-evaluation of silicon dioxide (E 551) as a food additive. *EFSA J.* **16**(1), e05088 (2018)
206. Athinarayanan, J., et al.: Presence of nanosilica (E551) in commercial food products: TNF-mediated oxidative stress and altered cell cycle progression in human lung fibroblast cells. *Cell Biol. Toxicol.* **30**(2), 89–100 (2014)
207. Peters, R., et al.: Presence of nano-sized silica during in vitro digestion of foods containing silica as a food additive. *ACS Nano* **6**(3), 2441–2451 (2012)
208. Taylor-Pashow, K.M.L., et al.: Hybrid nanomaterials for biomedical applications. *Chem. Commun.* **46**(32), 5832–5849 (2010)
209. Wang, L., Zhao, W., Tan, W.: Bioconjugated silica nanoparticles: development and applications. *Nano Research* **1**(2), 99–115 (2008)
210. Shirshahi, V., Soltani, M.: Solid silica nanoparticles: applications in molecular imaging. *Contrast Media Mol. Imaging* **10**(1), 1–17 (2015)
211. Teoh, W.Y., Amal, R., Madler, L.: Flame spray pyrolysis: an enabling technology for nanoparticles design and fabrication. *Nanoscale* **2**(8), 1324–1347 (2010)
212. Wolf, M.: Immer eine Idee besser: Forscher und Erfinder der Degussa. *Degussa AG, Frankfurt am Main* (1998)
213. Garrett, P.: Defoaming. CRC Press, Boca Raton (1992)
214. EVONIK. AEROSIL® – Fumed Silica. <http://www.aerosil.com/product/aerosil/downloads/technical-overview-aerosil-fumed-silica-en.pdf>
215. Stöber, W., Fink, A., Bohn, E.: Controlled growth of monodisperse silica spheres in the micron size range. *J. Colloid Interface Sci.* **26**(1), 62–69 (1968)
216. Shimura, N., Ogawa, M.: Preparation of surfactant templated nanoporous silica spherical particles by the Stöber method. Effect of solvent composition on the particle size. *JMatS* **42**(14), 5299–5306 (2007)
217. Ow, H., et al.: Bright and stable core-shell fluorescent silica nanoparticles. *Nano Lett.* **5**(1), 113–117 (2005)
218. Arriagada, F.J., Osseo-Asare, K.: Phase and dispersion stability effects in the synthesis of silica nanoparticles in a non-ionic reverse microemulsion. *ColSu* **69**(2), 105–115 (1992)
219. Huang, X., et al.: The effect of the shape of mesoporous silica nanoparticles on cellular uptake and cell function. *Biomaterials* **31**(3), 438–448 (2010)
220. Diagnosis and initial management of nonmalignant diseases related to asbestos. *Am. J. Respir. Crit. Care Med.* **170**(6), 691–715 (2004)
221. Trewyn, B.G., Whitman, C.M., Lin, V.S.Y.: Morphological control of room-temperature ionic liquid templated mesoporous silica nanoparticles for controlled release of antibacterial agents. *Nano Lett.* **4**(11), 2139–2143 (2004)